

See discussions, stats, and author profiles for this publication at: <https://www.researchgate.net/publication/200655647>

Long and Oriented Single-Walled Carbon Nanotubes Grown by Ethanol Chemical Vapor Deposition

ARTICLE *in* THE JOURNAL OF PHYSICAL CHEMISTRY B · OCTOBER 2004

Impact Factor: 3.3 · DOI: 10.1021/jp0474125

CITATIONS

105

READS

31

4 AUTHORS, INCLUDING:



Brian White

Columbia University

12 PUBLICATIONS 711 CITATIONS

SEE PROFILE



Stephen O'Brien

City College of New York

126 PUBLICATIONS 7,810 CITATIONS

SEE PROFILE

Long and Oriented Single-Walled Carbon Nanotubes Grown by Ethanol Chemical Vapor Deposition

Limin Huang,^{†,‡} Xiaodong Cui,^{‡,‡} Brian White,^{‡,‡} and Stephen P. O'Brien^{*,†,‡}

Department of Applied Physics and Applied Mathematics, Department of Chemistry, and the Columbia Nanocenter (NSEC), Columbia University, New York, New York 10027

Received: June 15, 2004; In Final Form: August 13, 2004

We report the controlled chemical vapor deposition (CVD) growth of single-walled carbon nanotubes (SWNTs), using ethanol as the carbon feedstock and bimetallic CoMo-doped mesoporous silica (SBA16) as the catalyst. Ultralong (up to 4 mm) and horizontally aligned SWNTs can be grown directly on flat substrates or across slits (20–120 μm apart), and the orientation of the nanotubes is always parallel to the gas flow direction. The control of the growth direction and length also enables us to fabricate parallel nanotube arrays or two-dimensional networks on flat surfaces. The growth of the carbon nanotubes is relatively fast—it is attributed to the high reactivity of ethanol and high activity of the CoMo/SBA16 catalyst—and no doubt contributes to increased length and orientation control. Unlike previous procedures that have been used to grow well-oriented nanotubes, neither a strong external electrical field nor a fast-heating technique is required in this ethanol CVD process. Moreover, the as-grown SWNTs have a relatively narrow size distribution of 0.8–1.8 nm, which is a result of the narrow size distribution of the CoMo nanoparticles embedded in the mesoporous SBA16 silica.

Introduction

Because of their unique electrical, mechanical, electro-optical, and electromechanical properties, single-walled carbon nanotubes (SWNTs) have been regarded as attractive building blocks for future nanoscale electronic devices, such as field-emitting devices, field-effect transistors, single-electron transistors, and molecular sensors.^{1–5} Most of these applications will require the ability to grow or assemble SWNTs with control over the diameter, helicity, orientation, and length.^{5–19}

Generally, carbon nanotube-based devices can be prepared by either deposition of a nanotube suspension on substrates^{5–9} or by chemical vapor deposition (CVD) growth of individual nanotubes directly on substrates.^{10–16} The direct CVD growth can afford individual SWNTs with few structural defects, whereas SWNTs in suspension usually exist as bundles or single tubes with short lengths (on the order of less than a micrometer) and may have defects arising from post-synthetic destructive treatments. Therefore, the controlled CVD growth of SWNTs directly on substrates can be shown to have several advantages over methods that involve the deposition of SWNT suspensions.

A general CVD growth without any external guidance normally yields short (lengths up to tens of micrometers) and randomly oriented SWNTs.¹⁰ Recently, some progress has been made in the surface growth of SWNTs, in regard to control over their diameter and orientation.^{12–16} For instance, diameter control was obtained by depositing uniform and monodispersed nanoparticles on substrates as the catalyst,^{14,15} and the diameter of SWNTs was correlated with the size of the catalyst nanoparticles.^{20,21} Alternatively, control over the orientation of

SWNTs was achieved by introducing an external electric field during a CVD process, and the alignment effect is believed to originate from the high polarizability of the nanotubes.^{12,13} Nevertheless, neither fabricating a microelectrode array nor introducing a strong electric field during the CVD growth is easy, especially for the large-scale fabrication. More recently, a “fast-heating” process was reported that involved mechanically sliding the catalyst-coated substrate through the furnace. This allows the growth of ultralong (lengths on the order of millimeters) and well-oriented SWNTs directly on substrates via CVD from carbon monoxide (CO).¹⁶

Here, we report a simpler process that can achieve the similar controlled growth, in regard to orientation, length, and diameter, while neither the specific fast heating technique nor the guidance of an external electric field is required. Long (lengths up to millimeters) and horizontally oriented, high-quality SWNTs can be grown directly on substrates via a CVD process at relatively low temperatures, using ethanol as a carbon feedstock and bimetallic CoMo-doped mesoporous silica as a catalyst. This simple CVD process represents an advancement in controlled growth for the large-scale fabrication of nanotube-based devices.

Experimental Section

Our group used thermally stable mesoporous silica thin films (SBA series) with ordered pore structure and uniform nanoporous channel (2–6 nm) to control the growth direction and diameter of SWNTs.¹⁸ The controlled growth was confirmed by the use of another type of mesoporous silica (MCM41) with smaller nanopores (2–3 nm) as a template to grow uniform-diameter SWNTs.¹⁹ Recently, some new CVD processes have been added to the family of CVD methods for SWNT production. For example, alcohol CVD at reduced pressures (5–10 Torr) was reported to produce amorphous carbon-free SWNTs in a wide temperature range (550–900 °C) when using methanol

* Author to whom correspondence should be addressed. Telephone: 212-854-9478, 212-316-3132. Fax: 212-854-8257. E-mail: so188@columbia.edu.

[†] Department of Applied Physics and Applied Mathematics.

[‡] Department of Chemistry.

[#] Columbia Nanocenter.

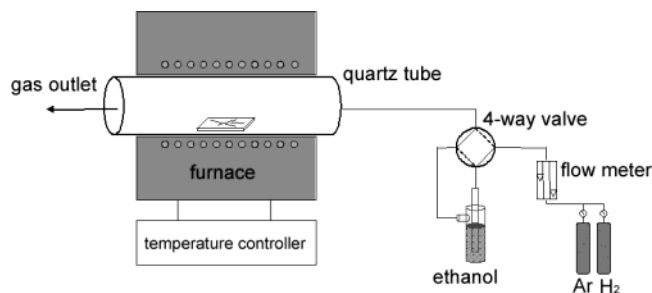


Figure 1. Schematic diagram of an ethanol chemical vapor deposition (CVD) setup. Ethanol liquid is kept in an ice bath (0 °C), and argon is bubbled into the ethanol through a four-way valve. The ethanol/argon mixture gas is delivered to the furnace, where the CVD is performed over a CoMo/SBA16 catalyst.

or ethanol as a carbon source.^{22–24} In addition, a so-called CoMoCat process was also reported to produce SWNTs with very narrow size and helicity distributions.^{17,25} Here, we take advantage of ethanol as the carbon source and bimetallic CoMo as the catalyst and then integrate them with the use of mesoporous silica, to devise a new ethanol CVD process that, as discussed later, shows great performance in SWNT growth with control over orientation, length, and diameter.

Preparation of CoMo-Doped Mesoporous SiO₂ Catalysts.

A mesoporous SBA16 silica precursor solution (three-dimensional (3D) mesoporous SiO₂, with a nanopore size of ~5.4 nm and pore openings perpendicular to the surface) was prepared by mixing tetraethoxysilane (TEOS), surfactant (Pluronic F127, EO₁₀₆PO₇₀EO₁₀₆), 0.1 M HCl, water, and ethanol at a molar ratio of 1:0.003–0.008:0.004–0.02:5–10:20–50, according to a previously reported procedure.^{18,26} A CoMo species then was incorporated into the mesostructure during a sol–gel process by mixing an ethanol solution of bimetallic precursors

Co(CH₃COO)₂ (Co(OAc)₂) and MoO₂Cl₂ or Mo(OAc)₂ (at a molar ratio of 1:0.3–1) with the SBA16 precursor solution (a molar ratio of CoMo/Si of 0.4%–1.5%).

With the catalyst precursor solution, it is easy to make CoMo/SBA16 catalysts in the form of thin films (via spin coating or dip coating) or various micropatterns (via photolithography or soft lithography) and easily place the catalysts at any desired location. The dried samples were then air-calcined at 550 °C for 2 h to acquire the 3D mesoporous structure that was embedded with the CoMo complex oxide nanoparticles.

The doping levels were controlled so that the mesoporous silica has a high thermal stability. Within certain doping levels, the silica matrix of the catalysts can retain the intrinsic mesostructure under CVD conditions.¹⁸ Because of the surface effect of the mesoporous silica, the active CoMo oxides can be well-dispersed in the mesostructure with the particle size confined by the channel dimension, which, in turn, controls the dimensions of the SWNTs. Furthermore, the mesoporous silica may act as a catalyst to help decompose ethanol, which is the carbon feedstock.

Catalyst Positioning Using Contact Microprinting. *p*-Type silicon wafers with an oxide layer 400 nm thick were used as substrates. A poly(dimethylsiloxane) (PDMS) stamp with a micropattern on the surface was first inked with a CoMo/SBA16 precursor solution. It was then placed in close contact with the substrate surface to transfer patterned catalysts onto the substrate. The dried samples were calcined in air at 550 °C for 2 h before CVD.

Ethanol Chemical Vapor Deposition Growth. The catalyst samples were placed in the middle of a 1-in.-diameter quartz tube furnace. Before the CVD, the catalysts were treated in an Ar/H₂ (350 sccm/50 sccm) flow during gradual heating and were reduced at the final CVD temperature (850 °C) for 10 min. After

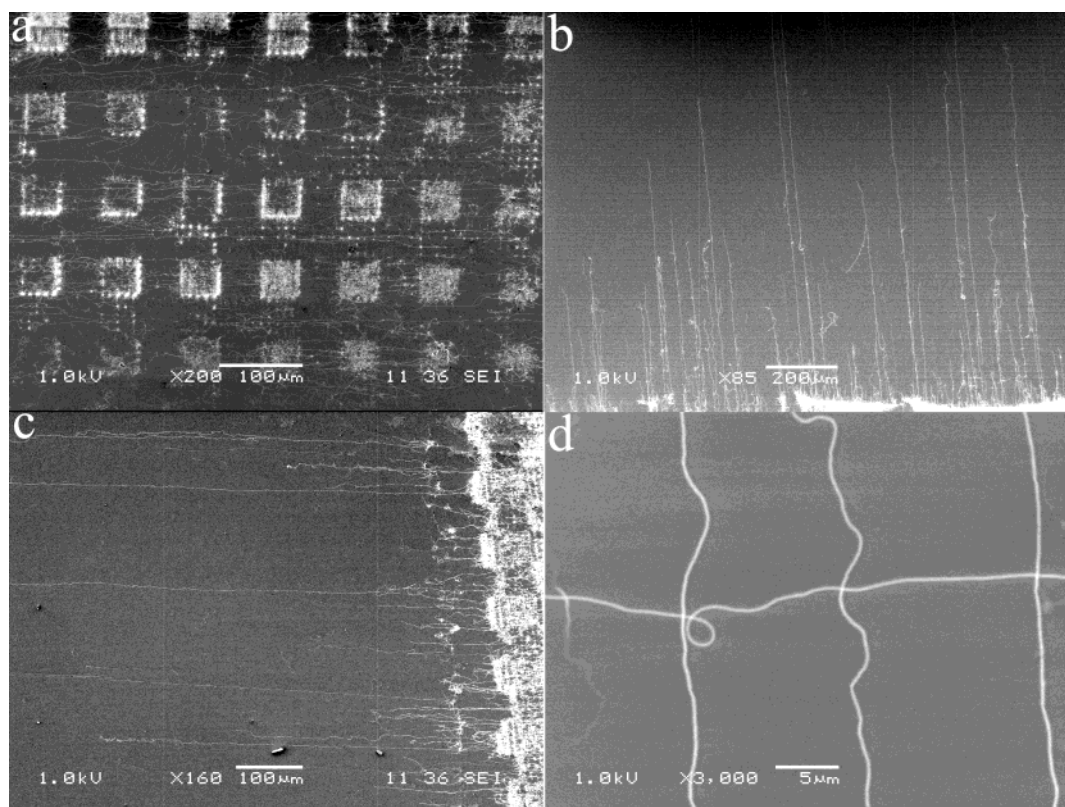


Figure 2. Typical scanning electron microscopy (SEM) images of (a) well-aligned nanotube arrays growing from micropatterned catalyst islands, (b, c) well-isolated, ultralong, and parallel nanotube arrays extending from the edge of the catalyst patterns with different orientations, and (d) cross junction of nanotube arrays by a two-step CVD growth.

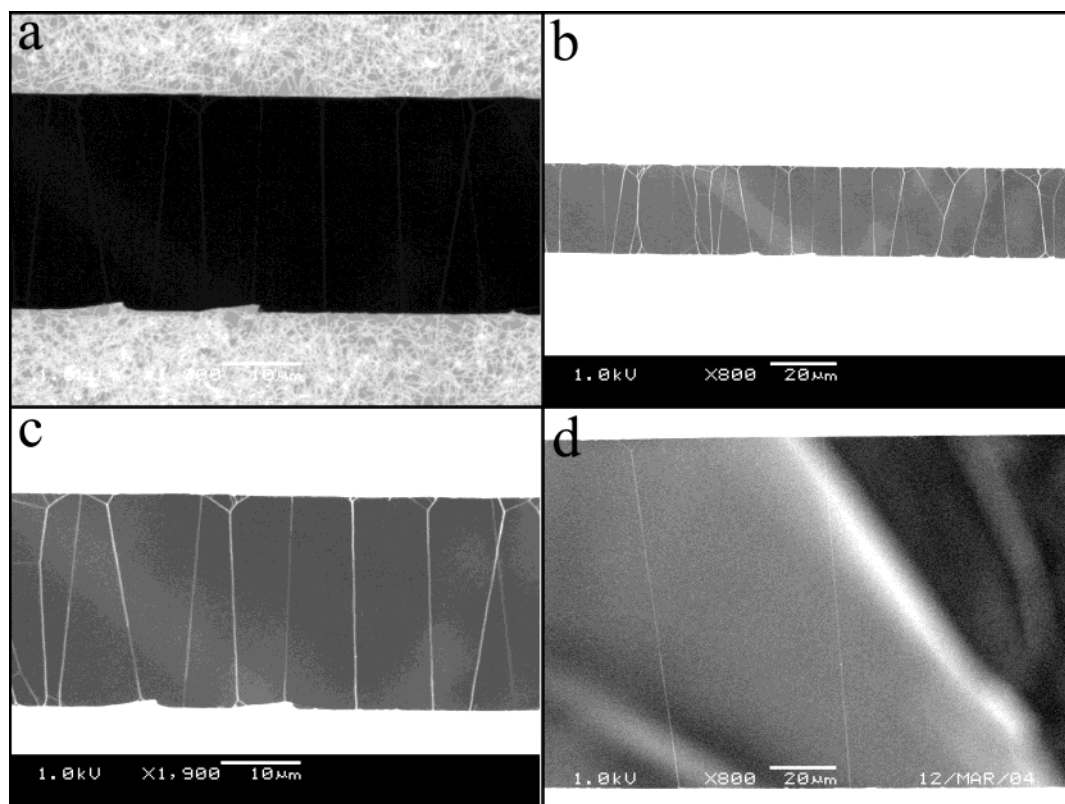


Figure 3. SEM images of suspended carbon nanotubes growing across slits with different gap distances ((a–c) $\sim 26 \mu\text{m}$ and (d) $\sim 120 \mu\text{m}$). Panels a and c show the same image with different contrast/brightness, highlighting random nanotube arrays growing on the surface (panel a), and a straight, almost-parallel nanotube array growing across the slit (panel c). Panel b is a low-magnification image of the sample in panel c. Panels b and d show that the densities of suspended carbon nanotubes across the slits decrease as the gap distance increases. The background in panels b and d results from the carbon tape underneath the slit, which is used to hold the sample in place for SEM analysis.

the reduction, ethanol vapor was delivered by bubbling argon (500–800 sccm) into a glass vacuum trap (outer diameter of 32 mm) containing ethanol (kept in an ice bath (0°C), with an ethanol vapor pressure of 11.8 mm Hg) through a four-way valve (see Figure 1). The ethanol/argon mixture was then transferred to the furnace, and the CVD was performed at 850°C for 20 min. It is quite different from the previous alcohol CVD method, in which alcohol vapor was delivered by a vacuum pump and the CVD was conducted under reduced pressure (5–10 mm Hg).^{22–24}

Characterization. Scanning electron microscopy (SEM) images were taken on a microscope (JEOL model JSM-5600LV) that was operated at 1 kV. Tapping-mode atomic force microscopy (AFM) images were taken on a Nanoscope IIIa (Digital Instruments), and the tube diameters were derived from the corresponding height measurement. Raman scattering analysis was performed by a confocal microscope that was equipped with a Trix spectrometer. The incident light from a HeNe laser (632.8 nm, 1 mW) was focused onto a $0.5\text{-}\mu\text{m}$ spot on the sample. Radial breath mode (RBM) spectra were collected using a liquid-nitrogen-cooled charge-coupled device (CCD) camera. Each RBM peak (ν_{RBM} , in units of cm^{-1}) corresponds to a specific tube diameter, which can be calculated based on the following equation:²⁷

$$d \text{ (nm)} = \frac{223.75}{\nu_{\text{RBM}} - 16}$$

Results

Oriented Single-Walled Carbon Nanotubes Grown from Micropatterned Catalyst Islands. Figure 2 shows the SEM

images of carbon nanotubes grown from the patterned CoMo/SBA16 catalysts (squares). Under observation via SEM, the carbon nanotubes appear as bright lines over a darker background. In Figure 2a, dense and randomly oriented nanotubes are found on each of the catalyst islands, and between the adjacent islands, there are almost parallel bridging nanotube arrays growing across. At the edge of the patterns, the well-oriented and isolated nanotubes keep growing in the direction of the flow and can extend to lengths of hundreds of micrometers and sometimes up to a few millimeters after 20 min of growth (Figure 2c). Figure 2b and c shows that directional control of parallel nanotube arrays can be obtained by orienting the substrate with respect to the gas flow direction. A cross connection of carbon nanotube arrays can be easily fabricated using a second CVD growth while changing the sample orientation, relative to the gas flow (Figure 2d). No additional catalyst was added for the second growth. We believe that a sufficient quantity of the catalyst was regenerated prior to the second growth, because of the presence of trace amounts of oxygen in argon.

The resulting individual nanotubes grown by our method are relatively straight. For some of the nanotubes, smooth curving morphologies such as S-shapes and loop shapes can be observed along the length of the tube, which may be due to local turbulent flow during the CVD (see Figure 2). Although further experimental and theoretical assessment of turbulent flow at these length scales is necessary, we attribute these coiled structural features in the nanotubes to the influence of the gas flow, which is consistent with previous observations.¹⁶

We found that the simultaneous growth of many nanotubes from within the catalyst islands results in a tendency for the

nanotubes to “interfere” with each other. This interference is the observation of a decrease in the linear directional growth and the interaction of tubes with each other, resulting in knotting or bundling of the tubes and an overall loss of control over orientation. This is due to their strong intermolecular forces of attraction. In contrast, we observe that nanotubes growing from the edge of the catalyst islands grow freely along the gas flow direction, leading to the formation of isolated and parallel nanotube arrays. In addition, it is worth mentioning that, in this ethanol CVD process, neither the fast heating technique nor the application of an external electric field is required to achieve controlled growth. Consistent with the previous results, the growth of ultralong and highly oriented nanotubes may result from their fast growth rates, which could ensure that the nanotubes quickly grow over the substrate along gas flow without significantly strong interactions with the underlying substrate.¹⁶

Suspended Carbon Nanotubes Growing across Slits. Our method can create parallel and straight nanotube arrays when they are grown across slits, as shown in Figure 3. Careful control over the deposition of the catalyst can easily result in isolated single-walled nanotubes suspended across slits with lengths that are dependent entirely on the slit gap, in the range of 20–200 μm . Such nanotubes are ideally suited for spectroscopy or electromechanical measurements that are important for fundamental physical characterization.

The slit samples were fabricated by photolithography with slits through the substrate. Each slit has a length of 2 mm and a width of 20–120 μm . The slit sample was dip-coated with a CoMo/SBA16 catalyst solution. After calcination, it was placed in the center of furnace with the long axis of the slit perpendicular to the gas flow direction. In Figure 3a, only short and randomly oriented nanotubes are found on the sample surface, because of the strong disturbance from neighboring nanotubes and/or van der Waals interactions with the surface. However, straight, well-oriented, and suspended nanotubes can be observed to grow across the slit (Figure 3b–d). Because the catalyst is deposited directly at the edge of the slit, the tubes start to grow from the edge of the slit. The nanotubes can grow parallel to the gas flow direction until they grow across the gap and come into contact on the opposite side of the slit. Because most of the growth starts from the edge of the slit, the chance of neighboring nanotubes growing together cannot be fully avoided. For the majority of the suspended nanotubes, a Y-shaped feature can often be found on both ends of the nanotubes, indicating that two or more neighboring nanotubes come close together and stick to each other to form small bundles. The suspended nanotubes appear very straight, because of undisturbed growth in the air, and they are free of van der Waals interactions with the surface. This is in contrast to the curving feature along the nanotubes when they are growing on a substrate surface.

The tube densities can be altered by changing the slit width. Figure 3b and d shows that well-oriented nanotube arrays can grow across the slits with gap distances in the range of 26–120 μm , although the tube densities decrease dramatically as the slit width increases. Longer nanotube arrays can barely be found across larger slits. In addition, the tube densities can also be controlled by the catalyst concentration and the CVD duration.

In the slit-growth experiment, most of the suspended tubes are observed to be small bundles with Y-shaped morphologies clearly visible via SEM on both sides of the slits, and only a small number of the suspended tubes are single tubes. We

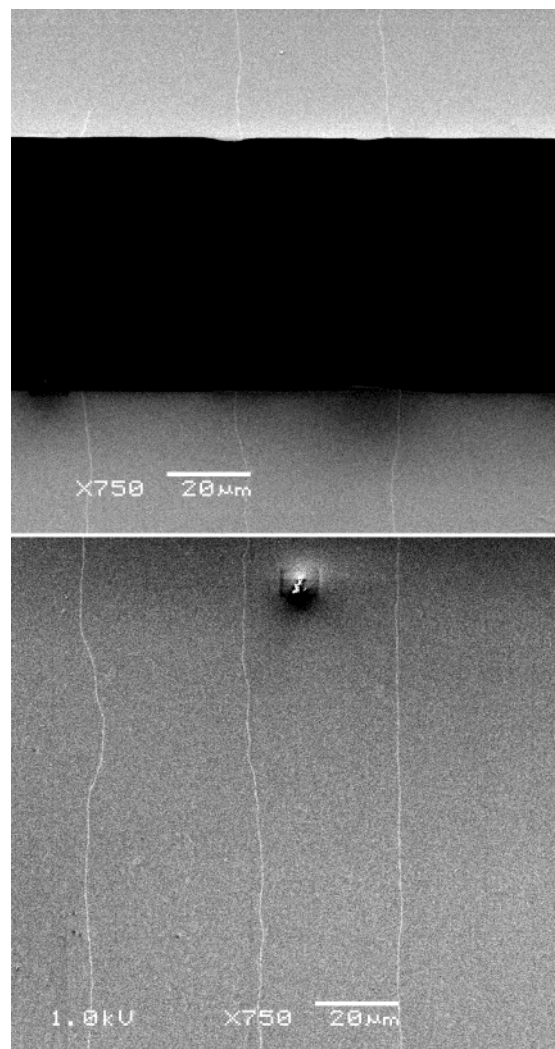


Figure 4. SEM images of individual carbon nanotubes growing across a slit sample. Nanotubes appear as white lines on a darker surface (SiO_2). The horizontal black region represents the slit ($\sim 60 \mu\text{m}$ in width) on the substrate surface. The catalysts were transferred onto the sample surface ~ 1 mm away from the edge of the slit by contact microprinting and the gas flow direction (pointing upward) is perpendicular to the slit direction.

suspect that this is typical for all procedures of this type. To obtain a single nanotube across the interface and avoid nanotube bundles or pairing, we used a contact printing technique: micropatterned catalysts were first transferred onto the surface of a slit sample with the pattern end ~ 1 mm away from the edge of slit. The samples were calcined and then placed in the center of the furnace with the direction of the slit perpendicular to the gas flow direction. After ethanol CVD growth at 850 $^\circ\text{C}$ for 20 min, the SEM images (Figure 4) show that carbon nanotubes can grow from the catalyst patterns and further extend outward onto the surface for a length of a few millimeters. In some cases, the longest tube can grow across the entire sample chip—that is, reach a length of ~ 4 –5 mm. As expected, these ultralong nanotubes follow the gas flow direction and grow across the slit (the black region in Figure 4, which represents the carbon tape underneath the slit sample, with a gap distance of $\sim 60 \mu\text{m}$). By changing the image contrast, the portion of the nanotubes that is suspended in the slit or trench can be observed as straight lines without pairing (no Y-shaped junctions). Nanotubes across the slit prepared by this method were confirmed to be individual tubes by optical measurements, which will be the subject of a future article. Even though neighboring

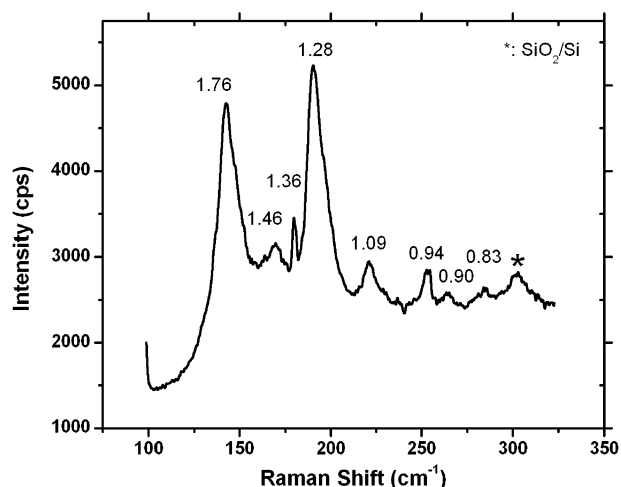


Figure 5. Typical Raman scattering (in the radial breathing mode (RBM) region) of as-grown carbon nanotubes. Tube diameters (in units of nanometers) are shown, with the corresponding peaks.

nanotubes stick together to form bundles initially, with this continuous growth method, the chances of the nanotubes in a bundle to grow at a similar pace decrease, so the small bundle eventually becomes a single tube. The ability of growing single tubes across slits/trenches is very important for the fundamental study of electric and optical properties at the single isolated nanotube level, as well as for device fabrication.

Control over Nanotube Diameter. We have shown that control over the tube position, length, and orientation can be achieved by our described ethanol CVD process. The process can also create SWNTs with a narrow size distribution and smaller diameter. Tapping-mode AFM showed that SWNTs extending from the catalyst patterns possessed diameters in the range of 1–1.2 nm. Larger-diameter nanotubes (e.g., 1.7 nm in diameter) were also observed but no tubes had diameters in excess of 1.8 nm (see Supporting Information). The long nanotubes are individual tubes other than small bundles. A relatively accurate measurement of the tube diameters results from their resonant Raman spectra (Figure 5), in which every radial breathing mode (RBM) peak corresponds to a specific tube diameter. In a typical Raman spectrum in Figure 5, the as-grown nanotubes have a relatively narrow size distribution of 0.8–1.8 nm. The two major tube diameters are ~1.28 and ~1.76 nm, respectively. There is also a small number of small-diameter nanotubes (<1 nm), with the smallest diameter being 0.83 nm, and few nanotubes >2 nm in diameter can be observed from the Raman spectra.

We believe that the small diameters and the relative narrow size distribution of the nanotubes are due to the small size of the catalyst nanoparticles embedded in mesoporous silica. As previously shown,²⁵ the combination of CoMo could result in tiny cobalt clusters (~1 nm) as catalysts and significantly reduce the formation of larger-size cobalt nanoparticles. On the other hand, because of the high surface area and the surface interactions between the catalyst nanoparticles and surface silanol groups, the mesoporous silica could act to prevent cobalt clusters from aggregating together to form larger nanocrystals at high CVD temperatures. This may contribute to the formation of small-diameter nanotubes with relative narrow size distribution.

Discussions

Unlike previous procedures used to grow well-oriented nanotubes, neither a strong external electrical field nor a fast-

heating technique is required in this ethanol CVD process. The fast growth of SWNTs is probably the reason for the control over length and orientation. A carbon source such as ethanol has higher reactivity than CO and methane (CH₄), because of a lower activation energy for ethanol decomposition. The CoMo-doped mesoporous silica catalyst is also highly active for the ethanol CVD growth. Not only are the CoMo oxides well-dispersed into the mesoporous structure and small in diameter, but the presence of surface Si–OH groups on mesoporous silica may help catalyze the decomposition of ethanol (e.g., dehydration reaction) at these reaction temperatures. As a result, the ethanol CVD permits a fast growth rate in regard to the growth of carbon nanotubes, even at a gradual heating rate, as opposed to fast heating. Thus, nanotube growth easily follows the gas flow without significantly strong interactions with the substrate surface and neighboring nanotubes, producing long, fairly straight tubes.

The fact that these long, single-walled nanotubes can grow across slits (tens of micrometers wide), and the fact that they grow parallel to the gas flow direction, suggests that during the CVD process, the nanotubes are being lifted upward and are caught in the laminar flow of the feeding gas above the surface. In previous observations of such phenomena, it has been argued that the catalyst is lifted off the surface and is carried by the gas flow, and the nanotubes grow via tip growth.¹⁶ The growth mechanism in our described method remains unclear, but it must be taken into consideration that the catalyst is embedded in the mesoporous host, which potentially favors a base-growth mechanism.

Conclusions

In summary, individual, long, and well-oriented single-walled carbon nanotubes (SWNTs) with relatively narrow size distribution can be grown directly on substrates or across slits by a chemical vapor deposition (CVD) process, using ethanol as the carbon feedstock and CoMo-doped mesoporous silica as the catalyst. The catalyst can be simply transferred using contact printing to the desired location, and thus positioning of the nanotubes can be controlled. Compared to conventional CO and CH₄ CVD for controlled growth, our ethanol CVD technique exhibits great advantages, in terms of its simplicity (no need for an electric field or a fast-heating technique) and ease of handling (less safety issues concerning the feedstock), which leads to the possibility of scaling up the reaction more easily. The advantages of the ethanol CVD controlled growth method will benefit the large-scale fabrication of nanotube-based devices and will facilitate the study of individual carbon nanotube characterization.

Acknowledgment. This work was supported primarily by the NSEC Program of the National Science Foundation (under Award No. CHE-0117752) and in part by the U.S. Department of Energy (under Grant No. DE-FG02-03ER15463) with additional support provided by the New York State Office of Science, Technology and Academic Research (NYSTAR). The work has used shared experimental facilities supported primarily by the MRSEC program of the National Science Foundation under award number DMR-0213574. We thank Dr. Henry X. Huang and Prof. James C. Hone of the Mechanical Engineering for supplying us with slit samples. We thank Prof. Ronald Breslow and Dr. Shalom Wind for useful discussions.

Supporting Information Available: AFM image of carbon nanotubes growing across a platinum electrode (PDF).

This material is available free of charge via the Internet at <http://pubs.acs.org>.

References and Notes

- (1) McEuen, P. *Phys. World* **2000**, *13*, 31.
- (2) Dai, H. J. *Surf. Sci.* **2002**, *500*, 218.
- (3) Misewich, J. A.; Martel, R.; Avouris, P.; Tsang, J. C.; Heinze, S.; Tersoff, J. *Science* **2003**, *300*, 783.
- (4) Ouyang, M.; Huang, J.-L.; Lieber, C. M. *Acc. Chem. Res.* **2002**, *35*, 1018.
- (5) Zhou, O.; Shimoda, H.; Gao, B.; Oh, S.; Fleming, L.; Yue, G.-Z. *Acc. Chem. Res.* **2002**, *35*, 1045.
- (6) Diehl, M. R.; Yaliraki, S. N.; Beckman, R. A.; Barahona, M.; Heath, J. R. *Angew. Chem., Int. Ed.* **2001**, *41*, 353.
- (7) Rao, S. G.; Huang, L.; Setyawan, W.; Hong, S. H. *Nature* **2003**, *425*, 36.
- (8) Chen, J.; Weimer, W. A. *J. Am. Chem. Soc.* **2002**, *124*, 758.
- (9) O'Connell, M. J.; Bachilo, S. M.; Huffman, C. B.; Moore, V. C.; Strano, M. S.; Haroz, E. H.; Rialon, K. L.; Boul, P. J.; Noon, W. H.; Kittrell, C.; Ma, J.; Hauge, R. H.; Weisman, R. B.; Smalley, R. E. *Science* **2002**, *297*, 593.
- (10) Kong, J.; Soh, H. T.; Cassell, A. M.; Quate, C. F.; Dai, H. J. *Nature* **1998**, *395*, 878.
- (11) Cassell, A. M.; Franklin, N. R.; Tomblor, T. W.; Chan, E. M.; Han, J.; Dai, H. J. *J. Am. Chem. Soc.* **1999**, *121*, 7975.
- (12) Zhang, Y. G.; Chang, A. L.; Cao, J.; Wang, Q.; Kim, W.; Li, Y. M.; Morris, N.; Yenilmez, E.; Kong, J.; Dai, H. J. *Appl. Phys. Lett.* **2001**, *79*, 3155.
- (13) Joselevich, E.; Lieber, C. M. *Nano Lett.* **2002**, *2*, 1137.
- (14) An, L.; Owens, J. M.; McNeil, L. E.; Liu, J. *J. Am. Chem. Soc.* **2002**, *124*, 13688.
- (15) Choi, H. C.; Kim, W.; Wang, D. W.; Dai, H. J. *J. Phys. Chem. B* **2002**, *106*, 12361.
- (16) Huang, S. M.; Cai, X. Y.; Liu, J. *J. Am. Chem. Soc.* **2003**, *125*, 5636.
- (17) Bachilo, S. M.; Balzano, L.; Herrera, J. E.; Pompeo, F.; Resasco, D. E.; Weisman, R. B. *J. Am. Chem. Soc.* **2003**, *125*, 11186.
- (18) Huang, L. M.; Wind, S. J.; O'Brien, S. P. *Nano Lett.* **2003**, *3*, 299.
- (19) Ciuparu, D.; Chen, Y.; Lim, S.; Haller, G. L.; Pfefferle, L. J. *Phys. Chem. B* **2004**, *108*, 503.
- (20) Cheung, C. L.; Kurtz, A.; Park, H.; Lieber, C. M. *J. Phys. Chem. B* **2002**, *106*, 2429.
- (21) Li, Y. M.; Kim, W.; Zhang, Y. G.; Rolandi, M.; Wang, D. W.; Dai, H. J. *J. Phys. Chem. B* **2001**, *105*, 11424.
- (22) Murakami, Y.; Miyauchi, Y.; Chiashi, S.; Maruyama, S. *Chem. Phys. Lett.* **2003**, *374*, 53.
- (23) Murakami, Y.; Yamakita, S.; Okubo, T.; Maruyama, S. *Chem. Phys. Lett.* **2003**, *375*, 393.
- (24) Maruyama, S.; Kojima, R.; Miyauchi, Y.; Chiashi, S.; Kohno, M. *Chem. Phys. Lett.* **2002**, *360*, 229.
- (25) Kitiyanan, B.; Alvarez, W. E.; Harwell, J. H.; Resasco, D. E. *Chem. Phys. Lett.* **2000**, *317*, 497.
- (26) Zhao, D. Y.; Yang, P. D.; Melosh, N.; Feng, J. L.; Chmelka, B. F.; Stucky, G. D. *Adv. Mater.* **1998**, *10*, 1380.
- (27) Yu, Z. H.; Brus, L. E. *J. Phys. Chem. B* **2001**, *105*, 6831.